Improved Limits on $\bar{\nu}_e$ Emission from μ^+ Decay

B. Armbruster,[1] G. Drexlin,[1] K. Eitel,[1] T. Jannakos,[1] J. Kleinfeller,[1] R. Maschuw,[1,3] C. Oehler,[1] P. Plischke,[1] J. Reichenbacher,[1] M. Steidl,[1] B. Zeitnitz,[1,5] H. Gemmeke,[2] M. Kleifges,[2] C. Eichner,[3] C. Ruf,[3] B. A. Bodmann,[4] E. Finckh,[4] J. Hößl,[4] P. Jünger,[4] W. Kretschmer,[4] J. Wolf,[5] N. E. Booth,[6] I. M. Blair,[7] and J. A. Edgington[7]

[1]*Institut für Kernphysik, Forschungszentrum Karlsruhe, 76021 Karlsruhe, Germany*
[2]*Institut für Prozessdatenverarbeitung und Elektronik, Forschungszentrum Karlsruhe, 76021 Karlsruhe, Germany*
[3]*Institut für Strahlen- und Kernphysik, Universität Bonn, Nußallee 14-16, 53115 Bonn, Germany*
[4]*Physikalisches Institut, Universität Erlangen-Nürnberg, Erwin-Rommel-Strasse 1, 91058 Erlangen, Germany*
[5]*Institut für Experimentelle Kernphysik, Universität Karlsruhe, Gaede-Strasse 1, 76128 Karlsruhe, Germany*
[6]*Department of Physics, University of Oxford, Keble Road, Oxford OX1 3RH, United Kingdom*
[7]*Physics Department, Queen Mary, University London, Mile End Road, London E1 4NS, United Kingdom*

(Received 14 February 2003; published 9 May 2003)

We investigated μ^+ decays at rest produced at the ISIS beam stop target. Lepton flavor (LF) conservation has been tested by searching for $\bar{\nu}_e$ via the detection reaction $p(\bar{\nu}_e, e^+)n$. No $\bar{\nu}_e$ signal from LF violating μ^+ decays was identified. We extract upper limits of the branching ratio (BR) for the LF violating decay $\mu^+ \to e^+ + \bar{\nu}_e + \overset{(-)}{\nu}$ compared to the standard model (SM) $\mu^+ \to e^+ + \nu_e + \bar{\nu}_\mu$ decay: BR $< 0.9(1.7) \times 10^{-3}$ (90% C.L.) depending on the spectral distribution of $\bar{\nu}_e$ characterized by the Michel parameter $\tilde{\rho} = 0.75(0.0)$. These results improve earlier limits by one order of magnitude and restrict extensions of the SM in which $\bar{\nu}_e$ emission from μ^+ decay is allowed with considerable strength. The decay $\mu^+ \to e^+ + \bar{\nu}_e + \nu_\mu$ often proposed as a potential source for the $\bar{\nu}_e$ signal observed in the LSND experiment can be excluded.

DOI: 10.1103/PhysRevLett.90.181804 PACS numbers: 13.35.Bv, 11.30.Hv, 14.60.Lm

Introduction.—In the standard model (SM), the main decay mode of positive muons is the decay into a positron and two neutrinos $\mu^+ \to e^+ + \nu + \nu'$. Assuming conservation of the additive lepton family or flavor (LF) numbers L_e and L_μ, the neutrino flavors are fixed to be $\nu = \nu_e$ and $\nu' = \bar{\nu}_\mu$. The neutrinos are massless with the ν_e being a left-handed neutrino and the $\bar{\nu}_\mu$ a right-handed antineutrino. The structure of the muon decay can be described by the *V-A* theory of weak interactions. Therefore, μ decay as a purely leptonic process has been used to study with high precision the SM of weak interactions. The Lorentzian *V-A* structure of the μ^+ decay can be tested by measuring the massive leptons, i.e., the initial μ^+ and the final e^+ [1] or by investigating the neutrino energy spectrum [2]. However, to test conservation of the LF numbers L_e and L_μ in μ decay, it is essential to observe the final neutrino states [3]. All tests so far show no deviations from the SM.

However, the LF number violating decay mode $\mu^+ \to e^+ + \bar{\nu}_e + \overset{(-)}{\nu}$ is allowed in many extensions of the SM, e.g., $\mu^+ \to e^+ + \bar{\nu}_e + \nu_\mu$ in left-right (LR) symmetric models [4–7], grand-unified-theory models with dileptonic gauge bosons [8], or supersymmetric models with R parity violation [9], together with the LF number violating decay $\mu^+ \to e^+ + \gamma$ [10,11], and $\mu^+ \to e^+ + \bar{\nu}_e + \bar{\nu}$ in extensions involving additional scalar multiplets [12]. Although the energy scale of LR symmetry of weak interactions or the appearance of supersymmetric particles is expected to be in the range of 0.1–1 TeV, precision measurements at intermediate energies can provide essential restraints on the parameters used in various models. Therefore, the detailed investigation of the μ^+ decay plays a major role in determining the structure of weak interactions and the precision of lepton number conservation.

On the other hand, there are clear evidences for neutrino oscillations from experiments on atmospheric, solar, and reactor neutrinos [13]. Since ν oscillations violate the conservation of the lepton family numbers, such results enhance the interest of searching for direct LF number violation. In addition, there is a positive $\bar{\nu}_e$ signal from the accelerator experiment LSND [14] which could be explained *a priori* as an indication for $\bar{\nu}_\mu \to \bar{\nu}_e$ oscillations of $\bar{\nu}_\mu$ from $\mu^+ \to e^+ + \nu_e + \bar{\nu}_\mu$ or directly for the decay mode $\mu^+ \to e^+ + \bar{\nu}_e + \overset{(-)}{\nu}$. Because of limited statistics and energy resolution, this ambiguity is not resolved by the LSND experiment itself.

The spallation source ISIS at the Rutherford Laboratory, U.K., is a unique source of μ^+ to study such decays. The Karlsruhe Rutherford Medium Energy Neutrino (KARMEN) experiment investigated the neutrinos produced at ISIS through the decays of π^+ and μ^+ at rest. One purpose of the KARMEN experiment was the investigation of ν-nucleus interactions on ^{12}C [15]. The good agreement of the measurements with theoretical predictions allowed a sensitive search for processes forbidden in the SM such as ν oscillations, $\nu_\mu \to \nu_e$ and $\bar{\nu}_\mu \to \bar{\nu}_e$ in the appearance mode [16] and $\nu_e \to \nu_x$ in the disappearance mode [17] or non-SM decay modes of π^+ and μ^+.

In this Letter, we report the results of the search for $\bar{\nu}_e$ from μ^+ decay at rest (DAR). Note that $\bar{\nu}_e$ from non-SM

interactions can be produced by either $\mu^+ \to e^+ + \bar{\nu}_e + \overset{(-)}{\nu}$ in the ISIS target or by oscillations $\bar{\nu}_\mu \to \bar{\nu}_e$ of $\bar{\nu}_\mu$ on their way to the detector with $\bar{\nu}_\mu$ being produced at ISIS in SM μ^+ decays. While the $\bar{\nu}_e$ energy spectrum is fixed in the DAR $\mu^+ \to e^+ + \bar{\nu}_e + \overset{(-)}{\nu}$ with a spatial flux according to a r^{-2} dependence, the energy and spatial distributions of $\bar{\nu}_e$ from oscillations strongly depend on the oscillation parameters, i.e., the mass difference $\Delta m^2_{ij} = |m^2_i - m^2_j|$. With its excellent energy resolution of $\sigma_E/E = 11\%/\sqrt{E[\mathrm{MeV}]}$, the KARMEN detector is able to separate different scenarios for potential $\bar{\nu}_e$ occurrence. Although the search for oscillations $\bar{\nu}_\mu \to \bar{\nu}_e$ and for the decay $\mu^+ \to e^+ + \bar{\nu}_e + \overset{(-)}{\nu}$ use the same detection reaction $p(\bar{\nu}_e, e^+)n$ for $\bar{\nu}_e$, the different physics and consequently the different e^+ spectral distributions result in two separate analyses.

$\bar{\nu}_e$ from LF violating μ^+ decays.—In the SM, applying the *V-A* theory, the energy spectra of massless neutrinos from μ^+ decay $\mu^+ \to e^+ + \nu_e + \bar{\nu}_\mu$ can be calculated neglecting radiative corrections as [18]

$$N(\epsilon)d\epsilon \propto \epsilon^2[3(1-\epsilon) + \tfrac{2}{3}\rho(4\epsilon - 3)]d\epsilon, \qquad (1)$$

with the relative energy $\epsilon = E_\nu/E_{\max}$, $E_{\max} = 52.83$ MeV for the decay at rest, and the Michel parameter $\rho = 0$ (0.75) for ν_e ($\bar{\nu}_\mu$), respectively.

Looking for physics beyond the SM, $\bar{\nu}_e$'s from $\mu^+ \to e^+ + \bar{\nu}_e + \overset{(-)}{\nu}$ in general have nonzero mass and contributions of left- or right-handed chirality eigenstates. As only the $\bar{\nu}_e$ in the decay $\mu^+ \to e^+ + \bar{\nu}_e + \overset{(-)}{\nu}$ is identified in the experiment, the second emitted (anti)neutrino $\overset{(-)}{\nu}$ is not determined. Since our experimental result sets upper limits on $\mu^+ \to e^+ + \bar{\nu}_e + \overset{(-)}{\nu}$, these limits also apply for the specific case $\overset{(-)}{\nu} = \nu_\mu$, which is the dominant one for certain model assumptions [5].

Taking the actual direct mass limits for $\bar{\nu}_e$, $m(\bar{\nu}_e) <$ 2.2 eV [19] (and hence for ν_μ and ν_τ masses through the mixing manifested in the experiments on neutrino oscillations), the ν masses are very small compared to the mass of the charged leptons or the energy scale of the neutrinos from μ^+ decays at rest. Assuming Majorana type neutrinos, the ν_e of left-handed chirality emitted in the SM decay $\mu^+ \to e^+ + \nu_e + \bar{\nu}_\mu$ could be detected via the reaction $p(\bar{\nu}_e, e^+)n$ since there is no distinction between ν_e and $\bar{\nu}_e$. However, the detection of $\bar{\nu}_e$'s emitted in muon decays with left-handed helicity would be strongly helicity suppressed $[1 - \beta \approx o(10^{-14})$ for a neutrino of 10 MeV energy and a rest mass of 2 eV/c^2] since only right-handed antineutrinos are absorbed via $p(\bar{\nu}_e, e^+)n$. In the case of Dirac type neutrinos, the above argument applies for left-handed chirality states of the $\bar{\nu}_e$ emitted. Therefore, current experiments are sensitive only to right-handed $\bar{\nu}_e$'s.

With the rest masses much smaller than the energy of all neutrinos emitted in $\mu^+ \to e^+ + \bar{\nu}_e + \overset{(-)}{\nu}$, an analytical description of the neutrino spectra similar to the one in Eq. (1) can be applied, with the spectral parameter $\tilde{\rho}$ to be specified, replacing the SM Michel parameter ρ. In some SM extensions with $\mu^+ \to e^+ + \bar{\nu}_e + \nu_\mu$, the $\bar{\nu}_e$ and ν_μ take the places of the SM $\bar{\nu}_\mu$ and ν_e, respectively, with $\tilde{\rho}(\bar{\nu}_e) = 0.75$ [5]. In others, $\tilde{\rho} = 0$ for the emitted $\bar{\nu}_e$ [12]. In our analysis, we therefore investigate the $\bar{\nu}_e$ emission for a variety of $\tilde{\rho}$ parameters.

Experimental configuration and data evaluation.—The experiment was performed at the neutrino source of the ISIS synchrotron accelerating protons to an energy of 800 MeV before striking a massive beam stop target. On average, 4.59×10^{-2} π^+ per incident proton are produced which are stopped within the target and decay at rest. Neutrinos emerge isotropically from the consecutive DARs $\pi^+ \to \mu^+ + \nu_\mu$ and $\mu^+ \to e^+ + \nu_e + \bar{\nu}_\mu$ [20] assuming the ν flavors of the SM decay channels. Neutrinos from μ^+ DAR have a continuous energy spectrum according to Eq. (1). Because of the narrow time structure of 525 ns of the proton pulses, muons are produced in a short time window compared to their lifetime of 2.2 μs.

The neutrinos are detected in a 56 t scintillation calorimeter [21] at a mean distance of 17.6 m from the ISIS target. The calorimeter is a mineral oil based scintillator segmented into 512 independent modules. Gadolinium within the module walls allows effective neutron detection via Gd(n, γ) in addition to the capture on the hydrogen of the scintillator via $p(n, \gamma)$. The scintillation detector provides an almost pure target of ^{12}C and ^{1}H for ν interactions. Three veto layers ensure a search for LF violating μ^+ decays almost free of cosmic background.

$\bar{\nu}_e$'s from μ^+ decay can be detected via the (e^+, n) sequence from charged current reactions $p(\bar{\nu}_e, e^+)n$ and $^{12}\mathrm{C}(\bar{\nu}_e, e^+n)^{11}\mathrm{B}$. Hence, the signature is a prompt e^+ and a delayed, spatially correlated γ signal from the capture of the thermalized neutron by $p(n, \gamma)$ with $E_\gamma = 2.2$ MeV or Gd(n, γ) with $\sum E_\gamma = 8$ MeV. The flux averaged [taking Eq. (1) with $\rho = 0.75$] cross section of $p(\bar{\nu}_e, e^+)n$ is $\sigma = 93.5 \times 10^{-42}$ cm^2 [22]. The $^{12}\mathrm{C}(\bar{\nu}_e, e^+n)^{11}\mathrm{B}$ contribution to (e^+, n) sequences has a cross section of $\sigma = 8.52 \times 10^{-42}$ cm^2 [23] which is further reduced relative to $p(\bar{\nu}_e, e^+)n$ by the abundance ratio H/C = 1.767 within the scintillator.

A positron candidate is accepted only if there is no activity in the central detector or in the veto system up to 24 μs beforehand. The prompt event is searched for in an interval of 0.6 to 10.6 μs after beam-on-target. The time structure of the prompt e^+ event relative to the proton pulses has to follow the μ^+ decay time constant of 2.2 μs. The expected visible e^+ energy has been simulated in detail based on $\bar{\nu}_e$ spectra with different values of the parameter $\tilde{\rho}$ including both detection reactions $p(\bar{\nu}_e, e^+)n$ and $^{12}\mathrm{C}(\bar{\nu}_e, e^+n)^{11}\mathrm{B}$. As a result, the prompt energy is required to be within 16 MeV $\leq E(\mathrm{prompt}) \leq$ 50 MeV (see Fig. 1). For further details of the data

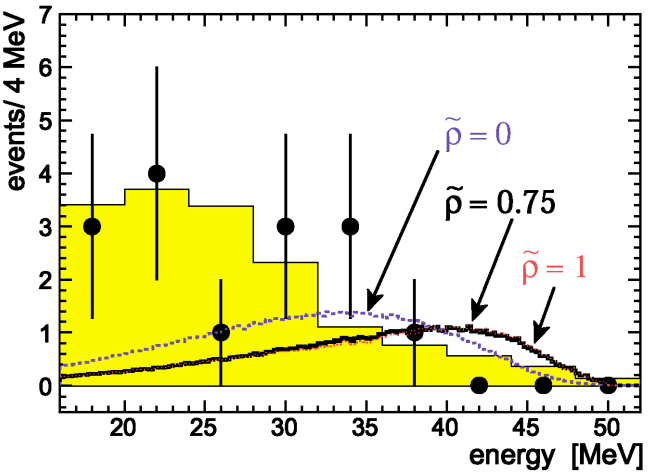

FIG. 1 (color online). Visible energy distribution of candidate events with background expectation (shaded area). The dashed and solid lines show the 90% C.L. limit for an additional $\bar{\nu}_e$ signal with a spectral parameter $\tilde{\rho} = 0$ and $\tilde{\rho} = 0.75$, respectively. The limit for $\tilde{\rho} = 1$ (dotted line) is experimentally almost indistinguishable from that for $\tilde{\rho} = 0.75$.

reduction of sequential event signatures and of the neutron detection in KARMEN, see also Ref. [16].

The raw data investigated in this search were recorded in the measuring period of February 1997 to March 2001 and represent the entire KARMEN 2 data set which corresponds to 9425 Coulombs protons on target with 2.7×10^{21} μ^+ decays in the ISIS target. Applying all evaluation cuts, 15 candidate sequences remain with prompt energies as shown in Fig. 1. The expected background amounts to 15.8 ± 0.5 events. This number comprises 3.9 ± 0.2 events from cosmic induced sequences as well as ν induced reactions such as intrinsic source contamination of $\bar{\nu}_e$ (2.0 ± 0.2), ν_e induced random coincidences (4.8 ± 0.3), and (e^-, e^+) sequences from $^{12}\mathrm{C}(\nu_e, e^-)^{12}\mathrm{N}_{\mathrm{g.s.}}$ with subsequent ^{12}N decay (5.1 ± 0.2). Except for the intrinsic $\bar{\nu}_e$ contamination, deduced from detailed Monte Carlo (MC) simulations, all the background components have been measured in different time and energy regimes with the KARMEN detector and extrapolated into the evaluation cuts applied for this $\bar{\nu}_e$ search.

Results and discussion.—The expected number of $\bar{\nu}_e$ induced events from $\mu^+ \rightarrow e^+ + \bar{\nu}_e + {}^{(-)}\nu$ is determined by the detection efficiencies of the prompt positron and the delayed neutron. The overall detection efficiency for positrons is given in Table I for a set of different spectral parameters $\tilde{\rho}$ including the contribution from $^{12}\mathrm{C}(\bar{\nu}_e, e^+n)^{11}\mathrm{B}$, which effectively amounts to less than 5% of the $p(\bar{\nu}_e, e^+)n$ signal in the energy interval of 16–50 MeV.

Based on the Poisson statistics of the numbers of candidate events and expected background, one can extract an energy-independent upper limit (90% C.L.) for an additional signal [24] of $N(\bar{\nu}_e) < 7.4$ excess events. However, there is additional spectral information, as can be seen from Fig. 1. To use this, we applied a maximum likelihood analysis varying the strength of a $\bar{\nu}_e$ signal with the energy distribution according to a set of different $\tilde{\rho}$ parameters. Table I shows the signal strength $N(\bar{\nu}_e)_{\mathrm{bestfit}}$ from the likelihood method. To extract 90% C.L. intervals for $N(\bar{\nu}_e)$, we performed large samples of MC simulations reproducing experimentlike spectra under different hypotheses. Our experimental result is consistent with no $\bar{\nu}_e$ emission from μ^+ decay with upper limits given in Table I, extracted within a unified frequentist analysis near the physical boundary $N(\bar{\nu}_e) = 0$ following Ref. [25].

Choosing a specific value, $\tilde{\rho}(\bar{\nu}_e) = 0.75$, a potential signal strength of $N(\bar{\nu}_e) = 5828 \pm 538$ for a branching ratio BR = 1 for LF number violating decays is expected. With $N(\bar{\nu}_e)_{90\%\mathrm{C.L.}} < 5.3$, an upper limit at 90% C.L. of the branching ratio of

$$\mathrm{BR} = \frac{\Gamma(\mu^+ \rightarrow e^+ + \bar{\nu}_e + \nu^{(-)})}{\Gamma(\mu^+ \rightarrow e^+ + \nu_e + \bar{\nu}_\mu)} < 9 \times 10^{-4} \qquad (2)$$

can be derived as well as the upper limits given in Table I for other values of $\tilde{\rho}(\bar{\nu}_e)$. Figure 1 shows the visible e^+ energies from $\mu^+ \rightarrow e^+ + \bar{\nu}_e + {}^{(-)}\nu$ for different $\tilde{\rho}$ parameters with total strength excluded at 90% confidence.

The above limits on the BR on μ^+ decays emitting $\bar{\nu}_e$ improve by more than an order of magnitude the most sensitive limit so far of $\mathrm{BR}(\mu^+ \rightarrow e^+ + \bar{\nu}_e + \nu_\mu) < 0.012$ obtained by the E645 experiment at LAMPF [24,26].

TABLE I. Flux averaged cross section $\langle\sigma\rangle$ for $p(\bar{\nu}_e, e^+)n$ and $^{12}\mathrm{C}(\bar{\nu}_e, e^+n)^{11}\mathrm{B}$, total efficiency for e^+ detection, expected (e^+, n) sequences for μ^+ decaying entirely via $\mu^+ \rightarrow e^+ + \bar{\nu}_e + {}^{(-)}\nu$, experimental results for potential $\bar{\nu}_e$-induced events, and deduced upper limits for the branching ratio for different spectral parameters $\tilde{\rho}$.

	$\langle\sigma\rangle[10^{-42}\ \mathrm{cm}^2]$		e^+ efficiency				
$\tilde{\rho}$	$\bar{\nu}_e + p$	$\bar{\nu}_e + {}^{12}\mathrm{C}$	[16–50] MeV	$N(\bar{\nu}_e)_{\mathrm{BR}=1}$	$N(\bar{\nu}_e)_{\mathrm{bestfit}}$	$N(\bar{\nu}_e)_{90\%\mathrm{C.L.}}$	BR (90% C.L.)
0.0	72.0	4.5	0.450	4304 ± 403	$+0.3$	<7.1	$<1.7 \times 10^{-3}$
0.25	78.8	5.8	0.452	4773 ± 445	-0.1	<6.2	$<1.3 \times 10^{-3}$
0.5	86.0	7.2	0.456	5273 ± 489	-0.4	<6.0	$<1.1 \times 10^{-3}$
0.75	93.5	8.5	0.462	5828 ± 538	-0.8	<5.3	$<0.9 \times 10^{-3}$
1.0	100.3	9.8	0.464	6272 ± 577	-0.8	<5.2	$<0.8 \times 10^{-3}$

In models extending the SM, the LF violating muon decay $\mu^+ \to e^+ + \bar{\nu}_e + \nu_\mu$ is often related to other LF violating processes, e.g., $\mu \to 3e$, $\tau \to \mu ee$, or muonium–antimuonium ($M\overline{M}$) conversion. Therefore, limits such as the limit on the probability for spontaneous conversion $P(M \to \overline{M}) < 8.2 \times 10^{-11}$ (90% C.L.) [27] allow one to set comparable, yet indirect, limits on the coupling constants responsible for the decay $\mu^+ \to e^+ + \bar{\nu}_e + \nu_\mu$ [5,28].

Even the most conservative upper limit of BR $< 1.7 \times 10^{-3}$ derived here for any value in the physically allowed range $0 \leq \tilde{\rho} < 1$ [1] is in direct experimental disagreement with the possibility that the beam excess of $\bar{\nu}_e$ seen in the LSND experiment is due to μ^+ decays with $\bar{\nu}_e$ emission with a probability of $P = (2.64 \pm 0.67 \pm 0.45) \times 10^{-3}$ [14]. For a quantitative comparison, one has to take into account that the LSND signal strength, interpreted either as branching ratio BR or oscillation probability P, has been derived under specific assumptions for the energy distribution of the $\bar{\nu}_e$. Furthermore, in the LSND maximum likelihood analysis of the data, excess events arise from $p(\bar{\nu}_e, e^+)n$ with $\bar{\nu}_e$ via $\bar{\nu}_\mu \to \bar{\nu}_e$ from μ^+ DAR as well as from $^{12}\mathrm{C}(\nu_e, e^-)^{12}\mathrm{N}$ with ν_e via $\nu_\mu \to \nu_e$ from π^+ decays in flight. The energy distribution of the prompt events is therefore a complex superposition of two excesses distorted by different L/E combinations from $\bar{\nu}_\mu \to \bar{\nu}_e$ and from $\nu_\mu \to \nu_e$ (up to 30% for large Δm^2), with L being the distance source detector and E the neutrino energy. For a detailed and complete comparison, one would therefore need a dedicated LSND analysis with respect to $\mu^+ \to e^+ + \bar{\nu}_e + {}^{(-)}\!\nu$ with different $\tilde{\rho}$ values as has been done here for the KARMEN data.

Nevertheless, quantitative statements can be deduced from straightforward extrapolations: The LSND excess corresponding to $\mathrm{BR}_{\mathrm{LSND}} = (2.64 \pm 0.67 \pm 0.45) \times 10^{-3}$ assumes $\tilde{\rho} = 0.75$ for the expectation with a branching ratio BR = 1 [[14], analog to the ratio in Eq. (2)]. Therefore, at 90% C.L., the limit $\mathrm{BR}_{\mathrm{KARMEN}} < 0.9 \times 10^{-3}$ can be directly compared with the lower limit from LSND assuming Gaussian errors $\mathrm{BR}_{\mathrm{LSND}} > (2.64 - 1.28\sqrt{0.67^2 + 0.45^2}) \times 10^{-3} = 1.6 \times 10^{-3}$ and leads to obvious inconsistency at more than 90% confidence for $\tilde{\rho} = 0.75$. For $\tilde{\rho} = 0$ with its lowest possible mean neutrino energy, the expected signal for BR = 1 decreases by about 35%, mainly due to the 33% reduction of the flux averaged cross section $\langle\sigma\rangle$ (see Table I). This reduction results from the change of the $\bar{\nu}_e$ energy spectrum and hence does not depend on experimental parameters. Since the LSND excess events remain unchanged, the extrapolated branching ratio for $\tilde{\rho} = 0$ increases to $\mathrm{BR}_{\mathrm{LSND}} = (3.5 \pm 0.9 \pm 0.6) \times 10^{-3}$ with $\mathrm{BR}_{\mathrm{LSND}} > 2.1 \times 10^{-3}$ (90% C.L.), to be compared with $\mathrm{BR}_{\mathrm{KARMEN}} < 1.7 \times 10^{-3}$ (90% C.L.). Comparisons for other values of $\tilde{\rho}$ lead to similar results.

We conclude that, at a confidence level of 90%, the derived KARMEN limits exclude the hypothesis of a $\mu^+ \to e^+ + \bar{\nu}_e + {}^{(-)}\!\nu$ decay signal to explain the LSND excess events, regardless of any possible value of $\tilde{\rho}$.

We acknowledge financial support from the German Bundesministerium für Bildung und Forschung, the Particle Physics and Astronomy Research Council, and the Council for the Central Laboratory of the Research Councils. We thank the Rutherford Appleton Laboratory and the ISIS neutron facility for their hospitality.

[1] W. Fetscher and H. Gerber, *Precision Tests of the Standard Electroweak Model* (World Scientific, Singapore, 1993).
[2] B. Armbruster *et al.*, Phys. Rev. Lett. **81**, 520 (1998).
[3] P. Langacker and D. London, Phys. Rev. D **39**, 266 (1989).
[4] R. Mohapatra and J. Pati, Phys. Rev. D **11**, 566 (1975).
[5] P. Herczeg, Z. Phys. C: Part. Fields **56**, 129 (1992).
[6] P. Herczeg and R. N. Mohapatra, Phys. Rev. Lett. **69**, 2475 (1992).
[7] R. N. Mohapatra, Prog. Part. Nucl. Phys. **31**, 39 (1993).
[8] H. Fujii *et al.*, Phys. Rev. D **49**, 559 (1994).
[9] A. Halprin and A. Masiero, Phys. Rev. D **48**, R2987 (1993).
[10] B. de Carlos and P. L. White, Phys. Rev. D **54**, 3427 (1996).
[11] K. S. Babu *et al.*, hep-ph/0211068.
[12] K. S. Babu and S. Pakvasa, hep-ph/0204236.
[13] G. L. Fogli *et al.*, hep-ph/0212127, and references therein.
[14] A. Aguilar *et al.*, Phys. Rev. D **64**, 112007 (2001).
[15] B. Armbruster *et al.*, Phys. Lett. B **423**, 15 (1998).
[16] B. Armbruster *et al.*, Phys. Rev. D **65**, 112001 (2002).
[17] B. Armbruster *et al.*, Phys. Rev. C **57**, 3414 (1998).
[18] C. Bouchiat and L. Michel, Phys. Rev. **106**, 170 (1957).
[19] J. Bonn *et al.*, Nucl. Phys. B, Proc. Suppl. **110**, 395 (2002).
[20] R. L. Burman *et al.*, Nucl. Instrum. Methods Phys. Res., Sect. A **368**, 416 (1996).
[21] G. Drexlin *et al.*, Nucl. Instrum. Methods Phys. Res., Sect. A **289**, 490 (1990).
[22] P. Vogel and J. F. Beacom, Phys. Rev. D **60**, 053003 (1999).
[23] E. Kolbe, in *Proceedings of the 5th International Symposium on Nuclear Astrophysics, Volos, Greece, 1998* (Editions Frontières, Paris, 1998).
[24] K. Hagiwara *et al.*, Phys. Rev. D **66**, 010001 (2002).
[25] G. J. Feldman and R. D. Cousins, Phys. Rev. D **57**, 3873 (1998).
[26] S. J. Freedman *et al.*, Phys. Rev. D **47**, 811 (1993).
[27] L. Willmann *et al.*, Phys. Rev. Lett. **82**, 49 (1999).
[28] S. Bergmann and Y. Grossman, Phys. Rev. D **59**, 093005 (1999).